

Circularly polarized V-shaped dielectric resonator antenna

Original

Circularly polarized V-shaped dielectric resonator antenna / Singhwal, Sumer Singh; Kanaujia, Binod K.; Singh, Ajit; Kishor, Jugul. - In: INTERNATIONAL JOURNAL OF RF AND MICROWAVE COMPUTER-AIDED ENGINEERING. - ISSN 1096-4290. - 29:9(2019). [10.1002/mmce.21832]

Availability:

This version is available at: 11583/3003134 since: 2025-09-26T09:36:43Z

Publisher:

Wiley

Published

DOI:10.1002/mmce.21832

Terms of use:

This article is made available under terms and conditions as specified in the corresponding bibliographic description in the repository

Publisher copyright

Wiley postprint/Author's Accepted Manuscript

This is the peer reviewed version of the above quoted article, which has been published in final form at <http://dx.doi.org/10.1002/mmce.21832>. This article may be used for non-commercial purposes in accordance with Wiley Terms and Conditions for Use of Self-Archived Versions.

(Article begins on next page)

Circularly Polarized V-shaped Dielectric Resonator Antenna

Sumer Singh Singhwal¹, Binod Kumar Kanaujia², Ajit Singh³, Jugul Kishor⁴

¹Department of Electronics and Communication Engineering, Uttarakhand Technical University, Dehradun, India.

¹HMR Institute of Technology and Management, Delhi-110036, India.

²School of Computational and Integrative Sciences, Jawaharlal Nehru University, New Delhi-110067, India

³BTK Institute of Technology, Dwarahat, Uttarakhand, India

⁴Department of Electronics and Communication Engineering, National Institute of Technology, Delhi, India

Abstract- In this paper, a probe fed V-shaped dielectric resonator antenna (DRA) loaded with circular patches, is proposed for X band applications. A prototype was fabricated to validate the results. Circular polarization is achieved by the geometry of DRA integrated with the circular patches on its surface. These circular patches behave as a monopole antenna. To achieve circular polarization two orthogonal fields have been excited in the DRA which are in time phase quadrature. Due to the symmetry of design, it shows dual polarization, both LHCP and RHCP, in two orthogonal directions. The fabricated prototype exhibits wide impedance bandwidth of 7.85-10.1 GHz (25%) and circular polarization (CP) bandwidth of 8.35-8.7 GHz (4%). Maximum measured gain of 4.8 dBi has been obtained in comparison with the simulated gain of 5.6 dBi. Applications of the proposed antenna include satellite communication, telemetry tracking and control, Synthetic aperture radar (SAR), weather radar and military radar in X band. Directional CP performance is useful in designing a smart antenna and multiple input multiple output (MIMO) antenna.

Index Terms— Directional circular polarization, DRA, smart antenna, X band.

I. INTRODUCTION

The advent of efficient antennas has revolutionized the field of communication. In the pursuit of efficient antennas, in 1983 Long *et al.* [1-2] proposed cylindrical and rectangular dielectric resonator antennas (DRA). In 1984 Long *et al.* [3] presented hemispherical DRA. DRA is a relatively new concept of using dielectric material as antenna instead of metallic antennas which were used previously. Now a day, DRA antennas have been popular due to its various advantages over existing metallic antennas. Major advantages of DRA are wide impedance bandwidth as radiation area is more as compared to patch, low losses due to the dielectric body of the DRA, flexible excitation schemes as a number of options of excitation increases due to three-dimension body of the DRA, more design parameters (degree of freedom) and high radiation efficiency [4-7].

Circular polarization is also a much-sought property in antennas for satellite communication and radar applications due to low polarization losses, ease in the alignment of the antenna and ability to combat multipath interference and fading. The benefits of circular polarization in mobile services and communication are explained in [8-9]. Circular polarization can be achieved by single-feed, multi-feed and different DR shapes, however the mono feed method is easier

and compact. Different feed methods already discussed in the literature [4-5]. Initially, in the 1990s, basic geometrical shapes such as cylindrical and rectangular DRAs were studied at length [1-7]. Subsequently, different shapes of DRA were also analyzed such as trapezoidal [10], hexagonal [11], ring [12] and L-shaped [13] to achieve circular polarization. Pan *et al.* [10] discussed wideband circularly polarized trapezoidal DRA operating in 3-3.98 GHz band but, with a high volume of 16800 mm³. V. Hamasakutty *et al.* [11] discussed hexagonal shape DRA operating in 3-3.475 GHz band with 15% CP bandwidth. Mongia *et al.* discussed several shapes of DR including spherical, ring etc. in [12]. Shen *et al.* [13] discussed L-shaped DRA excited using Y-shaped microstrip line feed, operating in two bands with CP bandwidth 11.8-12.3 GHz and 14.3-14.8 GHz. And the quest for wide circular polarization and impedance bandwidth with different DRA structure is still pursued.

In this paper, V-shaped DRA is proposed for X band applications. A prototype of the proposed DRA is also fabricated to validate the results. Measured impedance bandwidth and measured axial ratio bandwidth (ARBW) of the proposed antenna are 25% (7.85-10.1 GHz) and 4% (8.35-8.7 GHz), respectively. This antenna can also be used in the MIMO antenna system and smart antenna array because of its

directional circular polarization property. Proposed antenna operates in X band which has a plethora of applications as discussed in [14-15] such as Radar and satellite communication. Smart beam steering antenna array is also one of the emerging applications in X band.

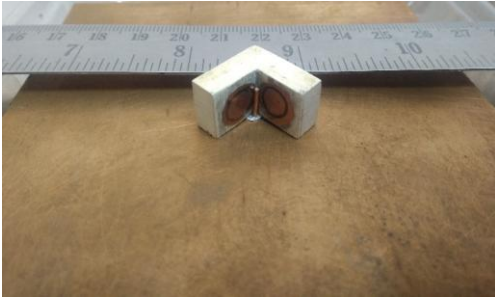


Fig. 1 Fabricated V-Shaped DRA Prototype

II. ANTENNA DESIGN

A. Antenna Configurations

In this paper, V-shaped DRA fed with the probe is proposed, as shown in Fig. 1. It comprises Eccostock Hik bar having relative dielectric constant 10 and its effective permittivity varies from 9.8-7 with respect to height of DRA from 1-11 mm, calculated using equation (4.29) of [16]. The Eccostock bar has been moulded in V-shape, a copper plate has been used as ground, two copper patches have been embedded on the surface of the DRA and a copper probe having diameter 1 mm has been used for feeding the structure. The schematic of the DRA is shown in Fig.2. Table-1 shows the dimensional details of the antenna. Antenna design steps are shown in Table-2.

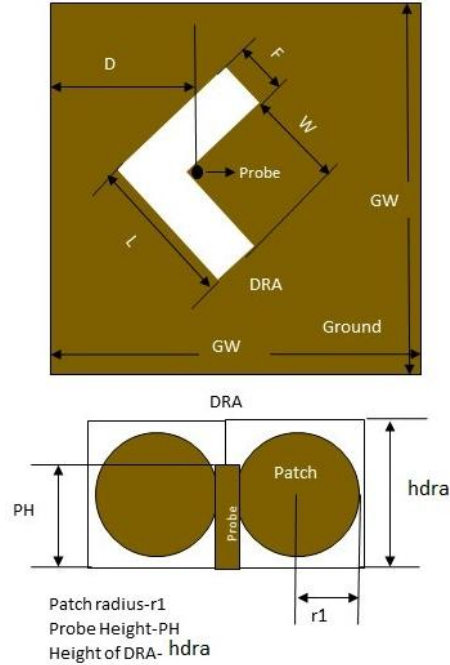


Fig. 2 Geometry of proposed DRA

Table-1

Design Parameters (in mm)							
L	W	F	hdra	r1	PH	D	GW
17	11	6	11.1	4.85	7.4	44	100

Table-2

Steps	Design	Impedance BW	ARBW
Step-1- RDRA		7.7-10.2 GHz	-
Step-2- V-Shaped DRA		9.2-9.6 GHz	9.08-9.12 GHz
Step-3- V-Shaped DRA with a single circular patch		8.25-9.8 GHz	-
Step-4- V-Shaped DRA with two circular patches		7.8-10 GHz	8.44-8.86 GHz

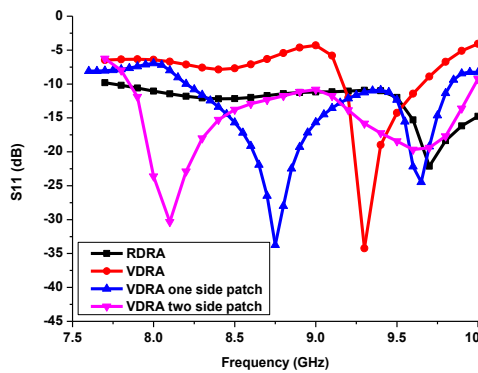


Fig. 3 Comparison of simulated impedance bandwidth of different antennas as shown in Table-2

In step-1, dimensions of the rectangular dielectric resonator antenna (RDRA) have been obtained using design equations (2-5), as mentioned by Mongia et al. [7]. Approximate parameter values obtained from design equations were further optimized using high-frequency structural simulator (HFSS). The dimension of the RDRA-1 is $6\text{ mm} \times 17\text{ mm} \times 11.1\text{ mm}$ which resonates at 9.6 GHz. In step-2, a V-shaped DRA is obtained by joining two RDRA and excited by a probe of diameter 1 mm at the center of the structure, as shown in Fig. 3. In the next step, a circular patch is etched on one surface of the V-shaped DRA which results dual resonance at 8.75 GHz and 9.65 GHz, as shown in the Fig. 3. Second resonance is due to circular patch etched on the surface of the DRA, having diameter $1.1\lambda_0/4$, where λ_0 corresponds to free space wavelength at resonant frequency 8.65 GHz. In the fourth step, two circular patches are etched on both sides of the DRA. These circular patches fed by probe are equivalent to monopole antenna as discussed in [17]. Consequently, the resonance frequency of the DRA shifts from 8.65 GHz to 8.1 GHz. Fig. 3 shows the comparison of simulated impedance bandwidths in all the steps explained above.

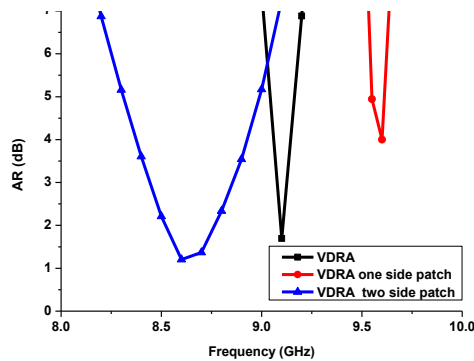
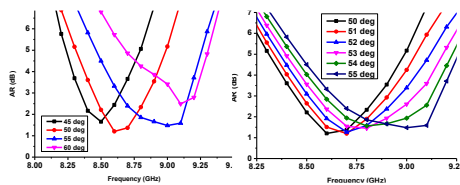


Fig. 4. Comparison of simulated AR of different antennas as shown in Table-2. All ARs are at $\theta=50^\circ$ and $\phi=50^\circ$

From the observation of the Fig.3, it is concluded that impedance bandwidth in step-1 is wide enough but ARBW is null. Step-2 aims to design a DRA with wide impedance bandwidth as well as pleasing ARBW. In this step, due to even symmetry in V-shape along the joint, DRA exhibits directional circular polarization. It shows RHCP at $\phi=50^\circ$ direction and LHCP at $\phi=-50^\circ$ direction. But the ARBW is still narrow, from 9.08-9.12 GHz (40 MHz), as shown in Fig. 4. To increase ARBW, in step 3 a circular patch was etched on one side of DRA which still results in diminished circular polarization due to asymmetrical structure. In step-4, ARBW has been increased from 40 MHz to 420 MHz by embedding two circular patches on both sides of the DRA, as depicted in Fig. 4. Fig-5 shows simulated AR for different elevation angles in coarser and finer views respectively. It is noticed that the minimum AR frequency point shifts w.r.t. the elevation angle. So, circular polarization is stronger at $\phi=\pm 50^\circ$ and $45^\circ < \theta < 55^\circ$.



(a) $\theta=45^\circ, 50^\circ, 55^\circ, 60^\circ$

(b) $\theta=50^\circ, 51^\circ, 52^\circ, 53^\circ, 54^\circ, 55^\circ$

Fig. 5. Simulated Axial Ratio Vs frequency variation for different values of elevation angle (θ) with a constant azimuth angle ($\phi=50^\circ$)

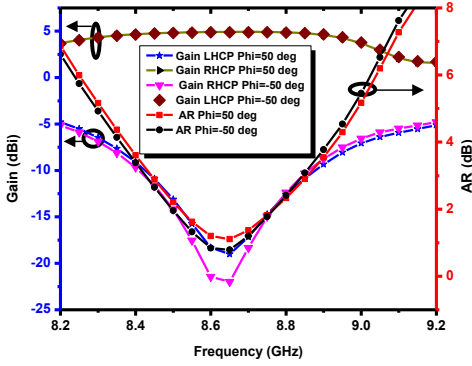


Fig. 6. Simulated Gain (LHCP and RHCP) and AR graphs in $\phi = \pm 50^\circ$ and $\theta = 50^\circ$ direction

Fig. 6 shows the comparison between gain (LHCP and RHCP) and axial ratios simulated for $\phi = \pm 50^\circ$ direction. Due to the symmetry of proposed antenna, gain (LHCP) at $\phi = -50^\circ$ and gain (RHCP) at $\phi = 50^\circ$ have approximately same values, gain (RHCP) at $\phi = -50^\circ$ and gain (LHCP) at $\phi = 50^\circ$ have also approximately same values. Simulated axial ratios in $\phi = \pm 50^\circ$ directions are also nearly same. Fig. 7 shows 3D radiation pattern plotted in XY plane and directions of circular polarization wave radiation with respect to antenna placement.

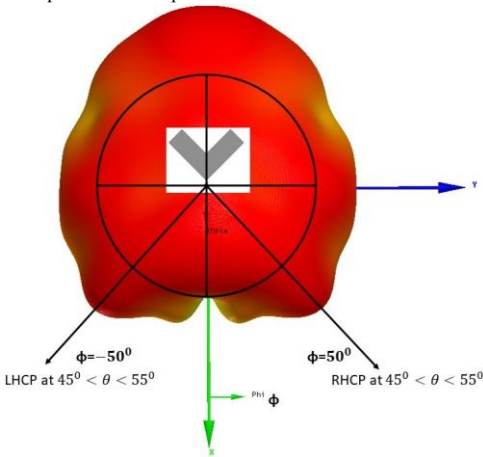


Fig. 7 3D radiation pattern in XY Plane showing the direction of RHCP and LHCP radiation at 8.65 GHz

Similarly, simulated impedance bandwidth and axial ratio bandwidth of the proposed design are 7.8-10 GHz (24%) and 8.44-8.86 GHz (5%) respectively, as shown in Fig. 3-4. The

Proposed DRA exhibits gain from 2.5-5 dB and good AR bandwidth in the range $45^\circ < \theta < 55^\circ$ at $\phi = \pm 50^\circ$. So, the proposed antenna demonstrates directional CP which can be used in smart beam steering antenna array system.

B. Effect of height of DRA

The height of any antenna plays a major role in its radiation properties. In case of DRA, bandwidth and mode degeneracy can be controlled by proper choice of resonator dimensions [5]. When the height of DRA varied it is observed that resonant frequency due to DRA also varied. To study the effect of the height of the proposed DRA, the design was simulated for four heights viz. 10 mm, 11 mm, 12 mm, 13 mm. S-parameters and axial ratio graphs are shown in Fig. 8 for various heights. The resonant frequencies and ARBW at various heights are tabulated in Table-3.

Table-3

Resonant frequencies at various heights of DRA		
Height of DRA (in mm)	Resonant Frequency (in GHz)	ARBW (in GHz)
10	9.7	8.12-8.22, 8.52-9.1
11	8.1 and 9.7	8.4-8.82
12	8.25 and 9.5	8.45-8.65
13	8.25 and 9.3	-

Alteration in surface current distribution and field distribution along the surface can be subtly observed due to the variation in the height of DRA. The orthogonal fields must have equal magnitude and must be in time phase quadrature for exciting circular polarization. Circular polarization depends on how effectively fields cross each other orthogonally. So, it is observed that when the height of DRA is 10 mm, circularly polarization is maximum but has poor impedance matching which can be improved by increasing the height of DRA to 11.1 mm.

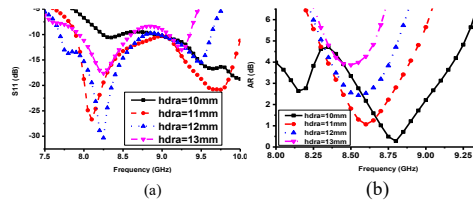


Fig. 8 Simulated S11 and AR against frequency for different heights of DRA. AR is at $\theta = 50^\circ$ and $\phi = 50^\circ$ (a) S11 (b) AR

However, the circular polarization is reduced a little bit but an improved impedance matching along the band is observed. Circular polarization further diminishes at 12 mm and 13 mm heights. Henceforth, circular polarization and impedance bandwidth are achieved at the optimized height of 11.1 mm, after observing its effects on different parameters.

C. Effect of the radius of circular patch

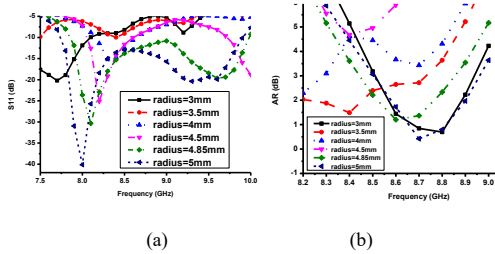


Fig. 9 Simulated S₁₁ and AR against frequency for different radius of patches etched on surfaces of DRA. AR is at $\theta=50^\circ$ and $\phi=50^\circ$ (a) S₁₁ (b) AR

Circular patch antennas can behave as a monopole antenna when etched on the surface of the dielectric substrate. Radiation properties of the monopole antenna change with respect to surface area and shape of the patch [17]. To study the effect of a change in surface area and size of the circular patch on radiation properties of DRA, the proposed antenna was simulated for different radii of the patch. Fig 9 shows the variation of S₁₁ and axial ratio against frequency for different radii of the patch. For radii less than 4 mm it has been found that excitation probe does not directly feed the circular patch, instead the energy has been coupled electromagnetically with the circular patch. Due to this, poor impedance bandwidth has been observed for radii less than 4 mm, as shown in the Fig. 9 (a). The resonant frequencies and ARBW at various radii are also tabulated in Table-4.

Table-4

Resonant frequencies at various radii of Patch		
Radius of Patch (in mm)	Resonant Frequency (in GHz)	ARBW (in GHz)
3	7.7	8.5-8.95
3.5	7.5	7.95-8.75
4	8.3	7.65-8.3
4.5	8.2 and 9.9	7.75-7.95
4.85	8.1 and 9.6	8.44-8.86
5	8 and 9.3	8.55-8.95

The resonance at 8.1 GHz is due to patch whose diameter corresponds to $\lambda_0/4$, where λ_0 is free space wavelength corresponding to resonant frequency. Table-4 shows increase in patch radius improves impedance bandwidth. Henceforth, circular polarization and impedance bandwidth are achieved at the optimized radius of 4.85 mm, after observing its effects on different parameters.

III. CHARACTERIZATION AND RESULT VALIDATION

The performance characteristics of the proposed DRA have been analyzed, investigated, and optimized by utilizing HFSS. A prototype of V-shaped DRA is fabricated with Eccostock HiK dielectric bar ($\epsilon_r=10$) as shown in Fig. 1. The circular

patch was cut down in shape manually by using copper foil tape of thickness 0.07 mm. Manual cutting with precise dimension is difficult at such a small scale. So, measurement was done using a circular patch on both sides having radius around 4.8 mm as shown in Fig. 1. This approximation of radius and manual fabrication results in concomitant imperfections which are slight dislocation of the circular patch on the DRA surface, soldering deformity and deposits, and adhesive applied for placing the DRA on the copper plate. These limitations produce variation in simulated and measured results which can be minimized in commercial fabrication.

Fig. 10 shows the comparison between simulated and measured results of impedance bandwidth and axial ratio. Simulated and measured impedance bandwidths of proposed DRA are 24% (7.8-10 GHz) and 25% (7.85-10.1 GHz) respectively. Simulated and measured axial ratio bandwidths of proposed DRA are 5% (8.44-8.86 GHz) and 4% (8.35-8.7 GHz) respectively. Measured results show agreement with simulated results with some variations due to manufacturing deformities. Fig-11 shows simulated and measured gain and simulated radiation efficiency of proposed DRA at $\theta=50^\circ$ and $\phi=50^\circ$. Maximum radiation efficiency is 94.5% and the maximum measured gain is 4.8 dBi in comparison to maximum simulated gain 5.6 dBi. Measured gain is less than simulated gain because of experimental approximations and fabrication deformities.

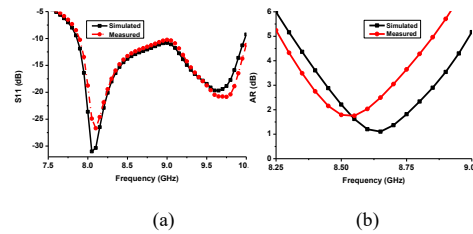
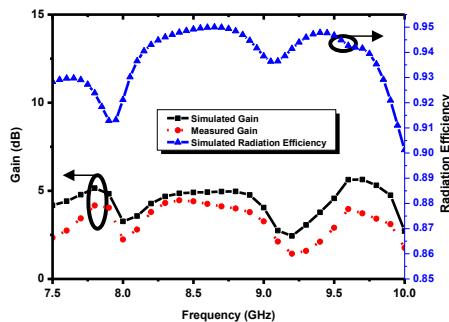


Fig. 10 Comparison of simulated and measured results (a) S₁₁ (b) AR DRA in $\theta=50^\circ$ and $\phi=50^\circ$ direction



Commented [VG1]: At 4 resonant frequency is 8.3 but in theory you write 8GHz, Similarly at 4.85 resonant frequency is 8.1 and 9.6 but theory you write at 4.8 radius resonant is 8.1. Similarly in fig 10(a) if you observe careful than first resonant is not id 8 . please verify all the frequency term you write in the paper and maintain uniformity.

Fig. 11 Simulated gain, measured gain and radiation efficiency at $\theta=50^\circ$ and $\phi=50^\circ$ of proposed V-shaped DRA

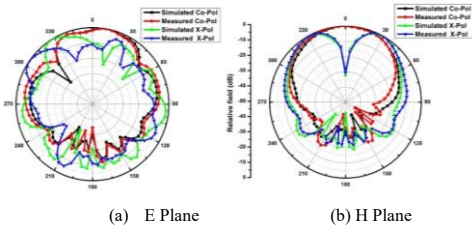


Fig. 12 Measured and simulated radiation pattern of the proposed DRA at 9.6 GHz frequency

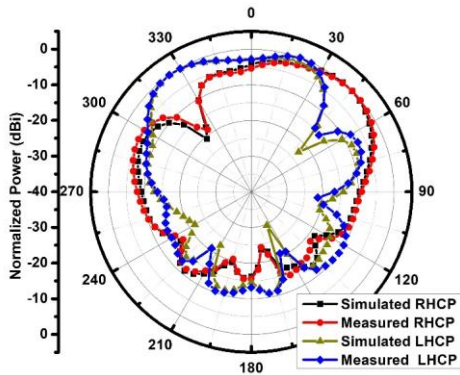


Fig. 13 Simulated and measured radiation pattern of the proposed DRA at 8.65 GHz and $\phi=50^\circ$ for circular polarization

Fig. 12 shows the radiation pattern at 9.6 GHz. The antenna exhibits linear polarization at 9.6 GHz. Fig. 13 shows gain (LHCP and RHCP) radiation pattern at 8.65 GHz. The antenna exhibits circular polarization at 8.65 GHz. Table-5 displays a comparison of proposed V-shaped DRA with recent circularly polarized DRAs operating in X band. Shen et. al [13] achieved 14% and 9.6% impedance bandwidth with 4% and 3% AR bandwidth using L-shaped DRA. Dash et. al [18] proposed dual-band circularly polarized triangular DRA with narrow AR bandwidth and low gain. Fakhte et. al [19] achieved high AR bandwidth of 6% using four stacked rotated rectangular DRAs. Kishk et. al [20] discussed elliptical DRA with 14% impedance bandwidth and 3.5% AR bandwidth. In comparison to these recent DRAs operating in X band, proposed fabricated DRA exhibits wide impedance bandwidth (25%) and pleasing AR bandwidth (4%).

An anechoic chamber is the most widely used electromagnetic measurement system. The results of the proposed antenna prototype have been measured in a rectangular shaped anechoic measurement chamber. A horn antenna has been

used as a reference antenna. The measuring antenna is placed in line with the reference antenna. The photograph of the anechoic measurement chamber is shown in Figure 14. Two-antenna method has been used to measure the axial ratio as explained in [21-22]. Receiving antenna is placed at Fraunhofer region in respect to the frequency of interest, from the transmitting antenna which is a fabricated prototype in this case. Anritsu vector network analyzer (MS2038C) that ranges up to 20 GHz has been used to measure S-parameters of the prototype.

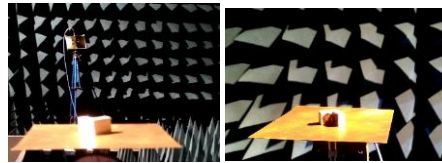


Fig. 14 Measurement setup in an anechoic chamber

Surface current movement at the surface of DRA is shown in Fig. 15, at different phase angles 0° , 90° , 180° and 270° . It shows RHCP movements of the current vector on DRA surface.

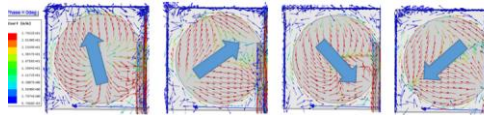


Fig.15. Simulated surface current at 8.65 GHz at different phase angles (0° , 90° , 180° , 270°)

Table-5 Comparison with recent DRAs operating in X band						
Ref.	DRA Shape	BW (%)	ARBW (%)	Gain (dBi)	Frequency (GHz)	Feed Type
[13]	L-shaped	14	4	-	11.9-13.7	Y shape Microstrip feed line
		9.6	3.4		14.9-16.4	
[18]	Triangular	12.37, 4.8	1.6, 1.8	2.15, 3.69	7.5,8.7	Probe feed
[19]	Rectangular	21	6	6.5	10	Aperture Coupled
[20]	Elliptical	14	3.5	-	9.4	Probe
Proposed	V-shaped	25	4	4.8	8.65GHz	Probe

IV. CONCLUSION

A wideband circularly polarized V-shaped DRA is presented in this paper. The maximum gain of the antenna is 4.8 dBi measured and 5.6 dBi simulated with pleasing circular

polarization bandwidth of 8.35-8.7 GHz. The antenna operates in 7.85-10.1 GHz band which lies in X band. The proposed antenna is equipped with various advantages like its compact design with the height of just 11 mm and volume 1848 mm³ with acceptable circular polarization and impedance bandwidth. The DRA falls in the category of the deserving candidate to be validated as compact design for it exhibits a directional circular polarization and a better average gain.

ACKNOWLEDGEMENT

Authors would like to acknowledge the Principal, G.B. Pant Engineering College Delhi, India, for providing antenna measurement facility at G.B.P.C.E. Delhi. Authors would like to thank the reviewers, for their valuable comments, which improved the quality of the manuscript.

ORCID

Sumer Singh Singhal¹  <https://orcid.org/0000-0002-8065-3284>
 Binod Kumar Kanaujia²  <https://orcid.org/0000-0002-7849-5299>
 Jugul Kishor⁴  <https://orcid.org/0000-0003-1108-998X>

REFERENCES

- [1] S. A. Long, M. W. McAllister, and L. C. Shen, "The resonant cylindrical dielectric cavity antenna," *IEEE Trans. Antennas Propagation*, vol. AP-31, no. 3, pp. 406-412, May 1983
- [2] M. W. McAllister, S. A. Long, G. L. Conway, "Rectangular dielectric resonator antenna," *Electron. Letters*, vol. 19, no. 6, pp. 218-219, Mar. 1983
- [3] M. W. McAllister and S. A. Long, "Resonant hemispherical dielectric antenna," *Electron. Lett.*, vol. 20, no. 16, pp. 657-659, Aug. 1984.
- [4] A. Petosa, *Dielectric Resonator Antenna Handbook*, Artech Publication House, 2007
- [5] K. M. Luk, K. W. Leung, Eds., *Dielectric Resonator Antennas*. Baldock, U.K.: Research Studies Press, 2003.
- [6] A. Petosa, A. Ittipiboon, "Dielectric Resonator Antennas: A Historical Review and the Current State of the Art" *IEEE Antennas and Propagation Magazine*, Vol. 52, No.5, 2010.
- [7] R.K. Mongia and A. Ittipiboon, "Theoretical and Experimental Investigations on Rectangular Dielectric Resonator Antennas", *IEEE Transactions on Antennas and Propagation*, Vol. 45, No. 9, September 1997.
- [8] J. L. Schadler, "Benefits of Circular Polarization for Mobile Services" available at http://www.dielectric.com/wp-content/uploads/2018/01/benifits_of_circular_polarization_for_mobile_services.pdf
- [9] S. S. Gao, Q. Luo, F. Zhu, "Introduction to Circularly Polarized Antennas" Wiley IEEE Press ISBN: 9781118790526
- [10] P Yongmei, L Kwok-Wa, "Wideband Circularly Polarized Trapezoidal Dielectric Resonator Antenna", *IEEE Antennas and Wireless Propagation Letters*, Vol. 9, pp 588-591, 2010.
- [11] V Hamsakutty, A.V.P Kumar, J Yohannan, et al., "Coaxial fed hexagonal dielectric resonator antenna for circular polarization", *Microwave and Optical Technology Letters*, Vol. 48, No. 3, pp 581-582, 2006.
- [12] R.K Mongia, A Ittipiboon, Cuhaci, et al. "Circularly polarised dielectric resonator antenna" *Electronics Letters*, Vol. 30 No. 17, pp. 1361-1362, 1994.
- [13] W. Shen, J. Liu, J Wu, K Yang, "Dual- band circularly polarized L-shaped dielectric resonator antenna" *International Conference on Electronics, Communications and Networks (CECNET IV)*, Beijing, China, 12-15 December 2014.
- [14] C. C. Schmillius & D. L. Evans, "Review article Synthetic aperture radar (SAR) frequency and polarization requirements for applications in ecology, geology, hydrology, and oceanography: A tabular status quo after SIR-C/X-SAR" *International Journal of Remote Sensing*. Volume 18, 1997 - Issue 13
- [15] W Huang et al. "Advances in Coastal HF and Microwave (S- or X-Band) Radars" *International Journal of Antennas and Propagation*, Oct. 2016.
- [16] R. Garg, P. Bhartia, I. Bahl, A. Ittipiboon, "Microstrip Antenna Design Handbook", Artech House, Norwood MA.
- [17] N.P. Agrawall, G. Kumar, K.P. Ray, "Wide-band Planar Monopole Antennas", *IEEE Transactions on Antennas and Propagation* 1998 ; 46(2): 294-295.
- [18] S.K. Dash et al, "Circularly Polarized Dual Facet Spiral Fed Compact Triangular Dielectric Resonator Antenna for Sensing Applications", *IEEE Sensors Letters Volume-2(3)*, 2017.
- [19] S. Fakhte, H. Oraizi and R. Karimian, "A Novel Low-Cost Circularly polarized rotated stacked dielectric resonator antenna," *IEEE Antennas and Wireless Propag. Lett.*, vol. 13, pp. 722-725, 2014
- [20] A. Kishk, "An elliptic dielectric resonator antenna designed for circular polarization with single feed", *Microwave and Optical Technology Letters*, 37(6), 454-456, 2003.
- [21] B.Y. Toh et al. "Understanding and measuring circular polarization" *IEEE Trans on Education*, Vol. 46, No. 3, August 2003.
- [22] *IEEE Standard Test Procedures for Antennas*, IEEE Standard 149, 1979 (R2008)